



Development of Multi-layer Tubular Vascular Scaffold to Enhance Compliance by Exhibiting a Negative Poisson's Ratio

Chi Bum Ahn¹ · Joo Hyun Kim² · Ji-Hyun Lee¹ · Kook Yang Park³ · Kuk Hui Son³ · Jin Woo Lee^{1,2}

Received: 30 September 2020 / Revised: 14 February 2021 / Accepted: 21 February 2021 / Published online: 8 April 2021
© Korean Society for Precision Engineering 2021

Abstract

Synthetic small diameter vascular grafts frequently fail owing to intimal hyperplasia, results from mismatched compliance between the vascular graft and native vessels. A vascular graft with a negative Poisson's ratio (NPR, materials expand transversely when pulled axially) was suggested to enhance compliance. We produced a three-layer tubular vascular scaffold with NPR properties. The luminal side consisted of nanosized electrospun fibers for endothelial cell (EC) growth. The middle layer was an NPR structure created using 3D printing, and the outer layer was a microsized electrospun fiber layer for vascular smooth muscle cell (VSMC) growth. The developed multi-layer tubular vascular scaffold contained NPR value. And the NPR vascular scaffold showed 1.7 time higher compliance than the PPR scaffold and 3.8 times higher than that of commercial polytetrafluoroethylene (PTFE) vascular graft. In addition, the ECs and VSMCs were well survived and proliferated on the scaffold during 10 days of culture. From the optimized co-culture condition of the VSMCs and ECs that VSMC phenotype changed was inhibited, we successfully generated a thin luminal layer, which consisted of ECs and the proper thickness of the VSMC layer under the ECs. This scaffold may have a potential to replace conventional artificial vascular graft by providing enhanced compliance and improved cell culture environment.

Keywords 3D printing · Compliance · Negative Poisson's ratio · Vascular scaffold · Co-culture

1 Introduction

Synthetic vascular grafts with a diameter < 6 mm are frequently occluded by thrombosis, aneurysms, or intimal hyperplasia [1, 2]. These complications are mainly caused by unmatched compliance which is inability to match

biomechanical behavior of a synthetic implant to that of an artery [3–5]. Therefore, the design feature of synthetic vascular grafts to increase compliance is critical. Compliance is a property that enables a body to resume its original size or shape when a distorting force is removed [3].

Poisson's ratio is the ratio of transverse contraction (expansion) strain to longitudinal expansion (contraction) strain in the direction of tensional (compressional) force [5]. Most natural materials are characterized by a positive Poisson's ratio (PPR) [6]. Thus, they contract laterally when stretched longitudinally. However, the classical theory of elasticity does not preclude the existence of materials with a negative Poisson's ratio (NPR), referred to as auxetics [7]. In comparison with traditional materials, auxetic systems have superior characteristics such as a higher resistance to indentation or larger fracture toughness [8]. Thus auxetic systems may be particularly useful for the development of vascular graft that contracts and expands due to blood flow [3]. In a previous study, an NPR sheet composed of photosensitive poly(ethylene) glycol diacrylate (PEGDA) was produced using projection stereolithography for 3D-printing [3]. Then, a tubular

Chi Bum Ahn and Joo Hyun Kim contributed equally this article as co-first authors.

✉ Kuk Hui Son
dr632@gilhospital.com

✉ Jin Woo Lee
jwlee@gachon.ac.kr

¹ Department of Molecular Medicine, College of Medicine, Gachon University, 155, Gaetbeol-ro, Yeonsu-ku, Incheon 21999, Republic of Korea

² Department of Health Sciences and Technology, GAIHST, Gachon University, Incheon, Republic of Korea

³ Department of Thoracic and Cardiovascular Surgery, Gil Medical Center, College of Medicine, Gachon University, 21, Namdong-daero 774 beon-gil, Namdong-gu, Incheon 21565, Republic of Korea

structure was created by rolling the sheet into a tube for a scaffold of vascular grafts. However, because the sheet fabrication and tube production were not simultaneously progressed at the same time in that technology, it took a lot of production time. Because photo-curable initiators were used, they are not free in terms of biological safety. Furthermore, the mechanical properties and compliance of the produced structure were not evaluated.

An understanding of the arterial structure is also essential to improve the mechanical properties of the vascular graft. An arterial wall is composed of three major layers: tunica intima, tunica media, and tunica adventitia [9]. The intima is comprised of a monolayer of endothelial cells (ECs). The media is composed of circumferentially arranged elastic fibers, vascular smooth muscle cells (VSMCs), and collagen fibers [9]. For increasing compliance, the main vascular cells, such as the ECs and VSMCs, should be properly accumulated as a layer, like the native vessels. Therefore, to create a proper layer, the scaffold for the vascular graft should have the ability to support the attachment, proliferation, and differentiation of vascular cells.

The electrospinning technology is attractive because it provides high mechanical durability, in terms of a high burst strength [1]. In addition, with the abundance of cell binding sites by large surface areas, electrospinning can promote the formation of a continuous monolayer of ECs in the lumen and proliferation of other cell types, such as VSMCs [1].

VSMCs have contractile or synthetic phenotypes [10]. Synthetic phenotype VSMCs can rapidly proliferate and produce an extracellular matrix (ECM), whereas those of the contractile phenotype maintain the function of the vascular media. The phenotype change of the VSMCs to the synthetic type induces intimal hyperplasia [10]. The cell-to-cell communication between ECs and VSMCs is critical for long-term patency by modulating the behavior and function of the blood vessels [10–13]. To maintain a contractile phenotype, the EC action on the VSMCs is important.

In this study, we designed a 3D printing system using a rotational stage to fabricate a tubular structure for a scaffold of an artificial vessel. To increase compliance and the responsiveness to blood pressure or flow changes, we aimed making tubular scaffolds having NPR properties. To compare compliance difference between NPR and PPR scaffolds, we designed this tubular scaffold with either NPR or PPR properties. We added electrospun fibers on the luminal and outer side of the scaffold to increase the mechanical durability and maximize cell adhesion and proliferation, and maintain cells own properties in the scaffold. With this scaffold, the regeneration of the EC and VSMC layers were attempted in the tubular structure using co-culture of the ECs and VSMCs.

2 Materials and Methods

2.1 Vascular Scaffold Fabrication

The vascular scaffold had 3 layers; most inner layer (luminal side) for EC seeding was made by electrospinning of polycaprolactone (PCL, (MW 45,000, Sigma-Aldrich, Germany), the medial layer was designed to have NPR or PPR and made by 3D printing of PCL, and the most outer layer for VSMC seeding was made by electrospinning of PCL (Fig. 1). To help a cell adhesion proper cell seeding, the luminal side electrospun layer was consisted of nano-size fibers and the outer side was consisted of micro-sized fibers. At first, the luminal side electrospinning was done with PCL on the 5 mm diameter brass rod which was rotated. With 3D printer, we fabricated NPR or PPR structure above the luminal electrospun layer during the rod rotation. On the 3D printing layer, we made then outer other layer of electrospun fibers with by a rod rotation.

2.2 Electrospinning

The electrospun fibers were deposited using an electrospinning device (NanoNC, Seoul, KOREA) on a rotating 5 mm diameter brass rod (Fig. 1). The rotating speed of the rod was 10 RPM. The flow rate of the electrospinning solution was 0.8 ml/h, and the distance between the spinning nozzle and rod was 60 mm. The operating voltage was 8–9 kV. To prepare the electrospinning solution, chloroform was blended with methanol indifferent ratios (1:1 or 4:1), and PCL (MW 45,000, Sigma-Aldrich, Germany) was dissolved in these mixtures at a 7.5% (w/w) concentration. For the nanosized electrospun fiber, a 1:1 ratio of chloroform and methanol was used. A 4:1 ratio of chloroform and methanol was used for the micro-sized electrospun fiber.

2.3 3D Printing for Made Scaffold Which had NPR or PPR

We created the medial layer having NPR and PPR properties using a 3D printer (Geo technology, Incheon, Korea). The 3D printer has 3 axis of X, Y and Z. A melted PCL polymer was extruded from the dispenser (Musashi Engineering Inc, Tokyo, Japan), which was attached on the Z-axis. A rotating rod connected to the W stage were modulated of a rotating speed by an independent controller. The rotation speed of W stage was 1 RPM to make a tubular NPR or PPR scaffold. PCL was melted in the printing dispenser at a temperature of 75 °C. PCL was extruded at 800 kPa as a filament through a heated metal micro-nozzle

Fig. 1 Fabrication process of the tubular vascular scaffold. **a** Rotating rod system. **b** Fabrication of a luminal layer with nanosized electrospun fibers. **c** Fabrication of a medial 3D printing layer with NPR and PPR patterns. **d** Fabrication of another layer with micro-sized electrospun fibers

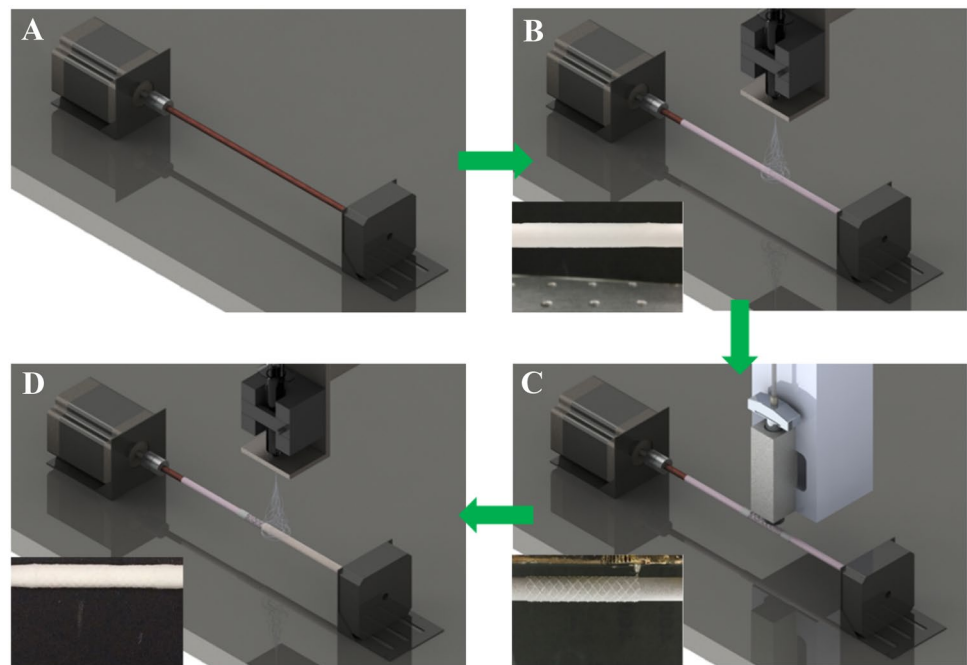


Table 1 Geometries of unit-cells

Reentrant honeycomb unit-cell (NPR)		$\zeta = 45^\circ$ $\gamma = 0^\circ$ $L_1 = 250 \mu\text{m}$ $L_2 = 250 \mu\text{m}$
Intact-rib unit-cell (PPR)		$\beta = 45^\circ$ $\gamma = 90^\circ$ $L = 250 \mu\text{m}$

(0.20 mm). The movement of the micro-nozzle along the X, Y, and Z axis were controlled using a CNC controller.

We selected the reentrant honeycomb unit-cell model to attain the NPR property and an intact-rib unit-cell design for PPR property based on previous studies [3, 14, 15]. The reentrant honeycomb meshwork showed various NPR magnitudes due to the dimensional variation of the structure. For example, changes of the central angles α and β result in the NPR effect. We designed the original angles as $\zeta = 45^\circ$ and $\beta = 0^\circ$ [3]. The intact-rib model was designed in a diamond shape and the properties of this model can be modulated by the values of angles β and γ , and we set $\beta = 45^\circ$ and $\gamma = 90^\circ$ in the present study [3] (Table 1).

2.4 Strain Test to Determine the Poisson’s Ratios

To measure Poisson’s ratios of tubular scaffold, strain tests were conducted. The tubular scaffold was loaded into an in-house strain measurement system. One end of vascular scaffold was fixed to Z axis of pulling device and the other end of vascular scaffold were fixed to the stage with jig. A tensile stress in the axial direction by the pulling motion of z axis was transferred to the end of a tubular scaffold. The Z axis of pulling device pulled the scaffold every 200 μm . The transverse and axial movements of the scaffold were recorded using a color CCD camera system (MST-101/7142, Beijing, China). In every time after 200 μm pooling of the scaffold, we recorded the transverse and axial deformation.

The overall transverse deformation of the scaffold caused by axial strains was used to calculate ν_{xy} , the Poisson’s ratios.

$$\nu_{xy} = -\frac{\epsilon_y}{\epsilon_x} \tag{1}$$

where, ϵ_y is transverse strain caused by an axial strain ϵ_x .

We calculated in-plane values of ν_{xy} caused by the strain on the unit cell. The expansion ratio was determined by the sum of contributions from the application of the incremental strains as:

$$\epsilon_i = \ln\left(\frac{L_i}{L_0}\right) = \sum_i \left[\ln\left(\frac{L_i}{L_{i-1}}\right) + \epsilon_{i-1} \right] \tag{2}$$

where, $i = 1, 2, 3, 4 \dots, n$ denote the current strain state, L_i is the specimen length for the current strain state i , and L_0 is the initial specimen length.

2.5 Measurement of the Tubular Scaffold Compliance

In order to evaluate the performance of the developed the Poisson's ratio tunable artificial blood vessel, a measurement of compliance is required. To measure the compliance, we used a balloon catheter with the maximum diameter of 7 mm (Ohicho II, Kaneka, Japan) and a pressure sensor (PS90030VY, Sentechnics, Italy) was used. And the pressure were by LabVIEW DAQ system. The measuring method was as follows. The thickness of a tubular scaffold was calculated by measuring the initial inner and outer diameter of the scaffold before applying the pressure. Then, a balloon stent was placed inside the tubular vascular scaffold and begins to apply the pressure. Considering the normal blood pressure of the artery, the outer diameter of the scaffold was measured by applied pressure of 80 mmHg (lower pressure) and 120 mmHg (higher pressure). The inner radius required for the compliance calculation was obtained using the following equation.

$$R_p = \frac{D_p}{2} - t$$

R_p = inner diameter at the applied pressure,

D_p = outer diameter at the applied pressure,

t = wallthickness

In addition, percentage compliance was acquired by the following equation.

$$\% \text{ compliance} = \frac{(R_{p2} - R_{p1})/R_{p1}}{P_2 - P_1} \times 10^4$$

P_1 = lower pressure (mmHg) = 80mmHg,

P_2 = Higher pressure (mmHg) = 120mmHg

2.6 Cell Culture

Cells were purchased and all methods were carried by relevant guidelines. Human VSMCs were purchased from the American Type Culture Collection (ATCC; No.CRL-1999). Human VSMCs were cultured in Dulbecco's Modified Eagle Medium/Nutrient Mixture F-12 (DMEM/F12, Gibco, Waltham, MA, USA) containing 15% fetal bovine serum (FBS; Gibco, Waltham, MA, USA), and penicillin/streptomycin (P/S; Gibco, Waltham, MA, USA). HUVECs were purchased from ATCC (No.CRL-1730). HUVECs were cultured in endothelial cell growth

medium-2 (EGMTM-2, Bullet Kit from Lonza, Basel, Switzerland).

2.7 Live/Dead Assay

For cell seeding, scaffold was trimmed as diameter 5 mm of circular shape. VSMCs were seeded at a dense of 1.5×10^4 cell/scaffold on the outer side of scaffold in a 96-well plate and cultured for 1, 4, 7 and 10 days. HUVECs were seeded at a dense of 3×10^4 cell/scaffold on luminal side of scaffold in a 96-well plate and cultured for 1, 4, 7 and 10 days. A live/dead fluorescent solution of calcein-AM and EthD-1 was prepared according to the manufacturers instructed dilutions (Thermo Fisher, Waltham, Massachusetts, USA). Scaffolds were then submerged in the solution and incubated at 37 °C for 40 min before being washed in PBS (Gibco, Waltham, MA, USA) and observed using a fluorescent microscope (Zeiss LSM 510, Germany). To quantification of cell viability in scaffold regions, image J software was used to analyze staining of calcein-AM region in each scaffold.

2.8 Cell Proliferation Assay

For cell proliferation assay, cell culture was done as same as live/dead assay. Cell proliferation rate was measured using cell counting kit (CCK8; Dojindo, Kumamoto, Japan). VSMCs were seeded at a dense of 1.5×10^4 cell/scaffold in a 96-well plate and HUVECs were seeded at a dense of 3×10^4 cell/scaffold in a 96-well plate. After 1, 4, 7 and 10 days, 100 µl CCK-8 solution were added to each well and the cells were incubated at 37 °C for 2 h. The absorbance at 450 nm was measured using ELISA reader (VERSAmax, U.S).

2.9 Scanning Electron Microscopy (SEM)

The morphology of the scaffold was observed under scanning electron microscopy (SEM) (SU 8010, Hitachi, Tokyo, Japan). Briefly, the scaffolds were sputter-coated with gold (HummerTM 6.2, Anatech Ltd., Denver, NC, USA) to a thickness of 10–15 nm. Images were acquired using a conventional SEM operating at an accelerating voltage of 25 kV with a 15 cm working distance.

2.10 Immunocytochemistry

To evaluate the VSMC phenotype change during single cell culture, the VSMCs were seeded at a density of 3×10^4 cell/scaffold for 3, 5, and 7 days. After fixation of cultured scaffolds with 4% paraformaldehyde, blocking was achieved by incubating the cells for 60 min in 5% normal goat serum (Vector laboratories, Burlingame, CA) in PBS/0.3% Triton X-100 (Sigma, St. Louis, Missouri, USA).

The VSMC-seeded scaffolds were incubated overnight at 4 °C with α -SMA or non-muscle MHC antibodies (Abcam, Cambridge, UK) at a dilution of 1:100, washed twice in PBS, and incubation for 2 h with donkey mouse alexafluor 488-conjugated secondary antibodies (diluted at 1:500 in blocking solution; Abcam). After washing the cells with tris-buffered saline twice, the scaffolds were counterstained with 4',6-diamidino-2-phenylindole (DAPI (to visualize nuclei; Vector Laboratories)).

To evaluate co-culture effect to decrease VSMC phenotype changes, at first VSMCs were seeded on the scaffold. The next day, HUVECs were seeded and co-cells were cultured for additional 2, 4, and 6 days. Then, α -SMA or non-muscle MHC staining was performed. For the immunocytochemical analysis at the co-culture on the tubular scaffold, VSMCs were seeded and then HUVECs were seeded 3 days (72 h) after VSMC seeding. The α -SMA, or vWF antibodies (Abcam, Cambridge, UK) were used and DAPI stain was performed.

2.11 Statistical Analysis

All data are presented as mean \pm standard deviation. Statistical significance between 4 groups was determined by performing the ANOVA and multiple comparisons by Bonferroni analysis. Statistical significant between 2 groups

were determined by Student's t test. Means were calculated from the results of 3 independent samples. P values < 0.05 were considered statistically significant. The analysis was performed SPSS version 22 (IBM Corporation, NY, USA).

3 Results

3.1 Physical Properties of the Vascular Scaffolds

By combining electrospinning and 3D printing with polycaprolactone (PCL), we successfully fabricated a multi-layer tubular scaffold with a 5 mm diameter. The scaffold contained three layers: the luminal nanosized electrospun fiber layer for EC growth, medial 3D printed layer, and outer microsized electrospun fiber layer for VSMC growth (Fig. 2). The medial layer was designed to have NPR or PPR properties by 3D printing. The thickness of the luminal electrospun fiber layer was 200 μm , and the thickness of the 3D printed layer was 200 μm . The thickness of the outer electrospun fiber layer was 400 μm . The fiber diameter of the luminal electrospun layer was 690 ± 70 nm, and the mean pore size was 4.51 ± 1.49 μm . The fiber diameter of the outer electrospun layer was 4.06 ± 0.05 μm , and the mean pore size was 16.66 ± 5.20 μm . Because they were made of the same material, each of the three layers adhered well to

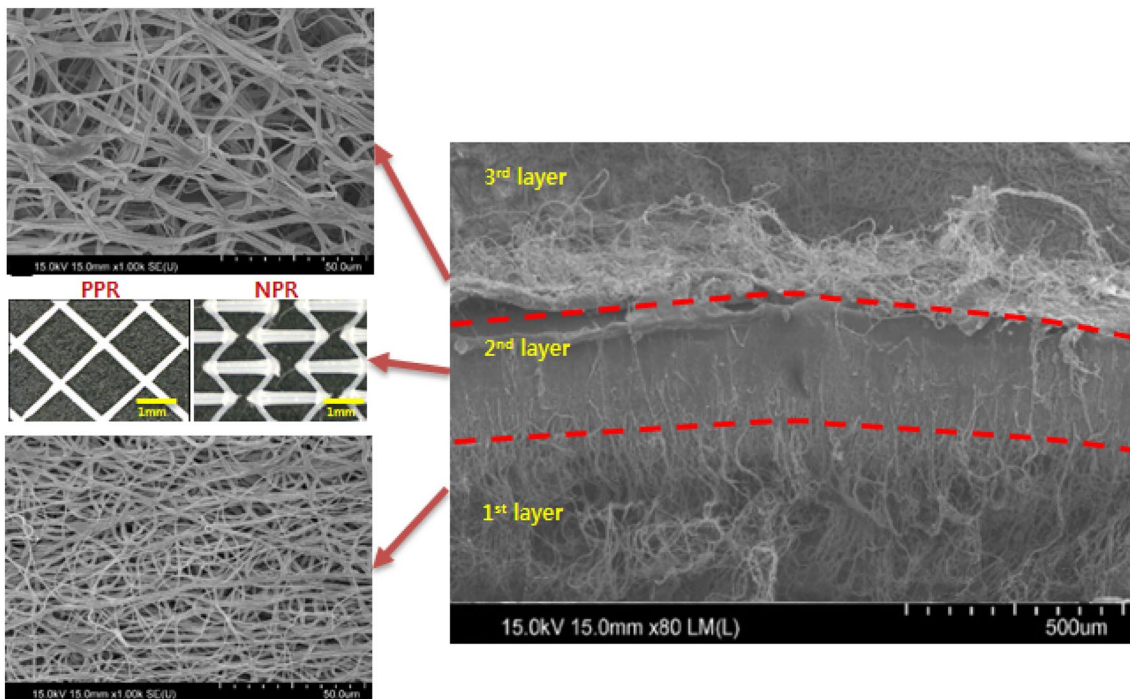


Fig. 2 SEM images of tubular vascular scaffold containing three layers. (The luminal layer consisted of nanofibers to seed ECs by electrospinning. The middle layer was fabricated to contain PPR or NPR

properties by 3D printing, and the outer layer consisted of microfibers to seed VSMCs by electrospinning)

each other. And, even though the contraction and expansion of the scaffold by the internal pressure change from 0 to 280 mmHg were repeated 20 times, the adhesion of each layer was maintained.

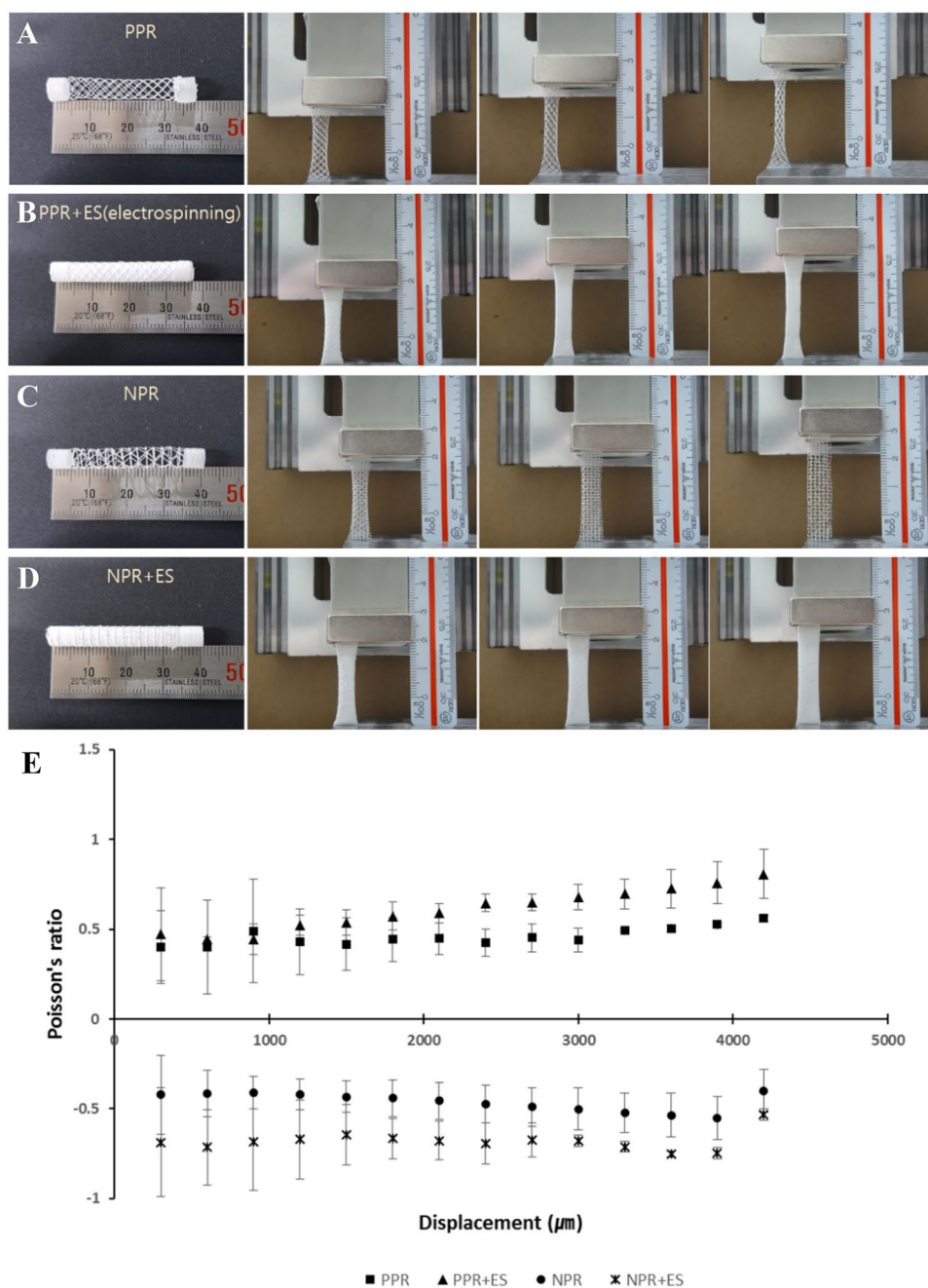
3.2 Poisson's Ratio of the Vascular Scaffold

We selected the reentrant honeycomb unit-cell model to obtain the NPR property and an intact-rib unit-cell design for the PPR property based on previous studies [3, 14]. The NPR or PPR properties of the tubular scaffold could change after electrospinning. To evaluate the change after

electrospinning, we compared the Poisson's ratio of the multi-layer tubular scaffold to a tubular scaffold with a 3D printed single layer (Fig. 3). The single and multi-layer PPR scaffolds showed PPR behaviors (Fig. 3a and b). In the elastic deformation range, the single layer PPR scaffold had a Poisson's ratio of 0.401–0.565, and the multi-layer PPR scaffold had a Poisson's ratio of 0.443–0.822 (Fig. 3e). The PPR behavior of the multi-layer PPR scaffold was similar to the single layer PPR scaffold.

The NPR scaffold showed NPR behavior (Fig. 3c and d). The single layer NPR scaffold had a Poisson's ratio of -0.551 to -0.401 , and the multi-layer NPR scaffold had a

Fig. 3 NPR or PPR properties of the scaffold when scaffolds were pulled axially by length of every 300 μm . **a** Expansion test of the single layer PPR scaffold. **b** Expansion test of the multi-layer PPR scaffold with the electrospinning layer. **c** Expansion test of the single layer NPR scaffold. **d** Expansion test of the multi-layer NPR scaffold with the electrospinning layer. **e** Poisson's ratio graph of the various types of scaffolds



Poisson's ratio of -0.750 to -0.533 (Fig. 3e). Although the standard deviation among each experiment, both multi-layer NPR scaffolds and single layer NPR scaffolds showed negative Poisson's ratio characteristics as we expected.

3.3 Measurement of Compliance

A compliance was calculated by measuring the change in the outer diameter of the tubular scaffolds when the pressure was changed from 80 to 120 mmHg (Fig. 4). The NPR vascular scaffold was 3.47% compliance ($\%/mmHg \times 10^{-4}$), PPR vascular scaffold was calculated by 2.04% compliance ($\%/mmHg \times 10^{-4}$) (Fig. 4c). Compared to the polytetrafluoroethylene (PTFE) value of 0.9% compliance, which was the report of Tai et al., the NPR vascular scaffold was 3.8 times that of PTFE, and the PPR scaffold showed a value of 1.7 times that of PTFE [16]. Of course, scaffolds containing NPR patterns showed the higher compliance owing to self-expandable characteristics.

3.4 EC and VSMC Cell Adhesion

We observed the EC (Human umbilical vein endothelial cells, HUVEC) and VSMC adhesion separately on the scaffold using SEM. We trimmed the vascular scaffold to a circular-shaped sheet and seeded the cells. ECs were seeded on the luminal side, which consisted of nanosized fibers, and the VSMCs were seeded on the outer side, which consisted of microsized fibers. The VSMCs were well attached to the microsized electrospun fibers after 3 days of culture (Fig. 5a). The ECs were well attached to the nanosized electrospun fibers.

3.5 EC and VSMC Proliferation and Survival on the Scaffolds

We observed the EC and VSMC proliferation separately on the scaffold using a CCK8 assay (Fig. 5b). We trimmed the vascular scaffold to a circular-shaped sheet and seeded the cells. The ECs were seeded on the luminal side, and VSMCs were seeded on the outer side. During 10 days of culture, the EC proliferation increased with the culture time dependent on the scaffold. The proliferation of the VSMCs on the scaffold was significantly increased with the culture time. The EC and VSMC survivals were observed separately on the scaffold using a live/dead assay. During a culture time of 10 days, the both of ECs and VSMCs on the scaffold showed cell survivals of greater than 90%. (Fig. 5c and d).

3.6 Evaluation of the Co-culture Condition of the ECs and VSMCs to Maintain the VSMC Phenotype on the Scaffolds

We evaluated the VSMC phenotypes on the scaffold trimmed to a circular shape. An alpha-smooth muscle actin (α -SMA) stain was used to detect the contractile type, and non-muscle myosin heavy chain (MHC) was used to detect the synthetic type (Fig. 6a and b) [17]. When we performed the single cell culture of the VSMC, synthetic-type VSMCs appeared at day 5 of the culture, and these were significantly increased at day 7 of culture (Fig. 6c and d).

To confirm the co-culture effect, which affected the phenotype change, we performed a co-culture of VSMCs and ECs (Fig. 6c and d). First, we seeded the VSMCs, then the ECs were seeded 1 day after VSMC seeding. And we evaluated the synthetic-type VSMCs at 3, 5, and 7 days from the culture start. The synthetic-type VSMCs appeared at 7 days of culture. Compared to the single cell culture of the VSMCs, the time point for the appearance of the synthetic type was delayed by the co-culture with ECs (Fig. 6c and d).

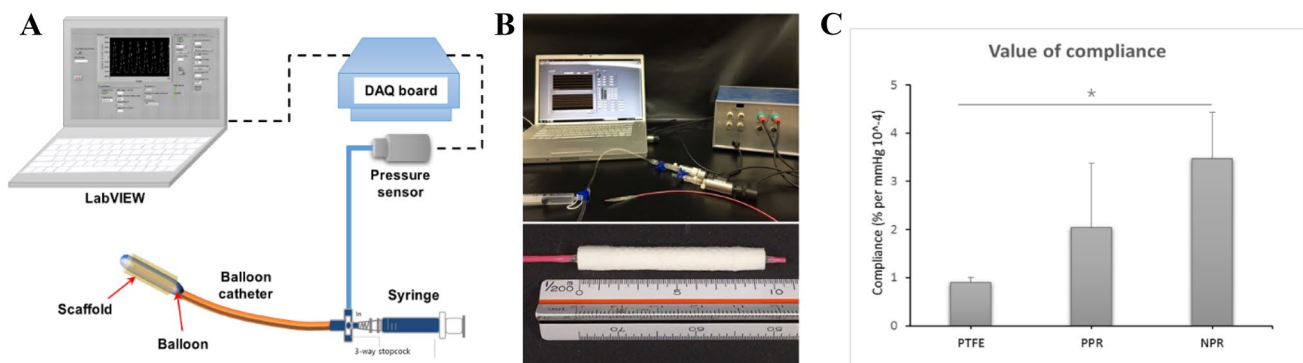


Fig. 4 Compliance measurement results. **a** Schematic diagram of the compliance measurement system, **b** Set-up of the compliance measurement system, **c** measurement results of the compliance

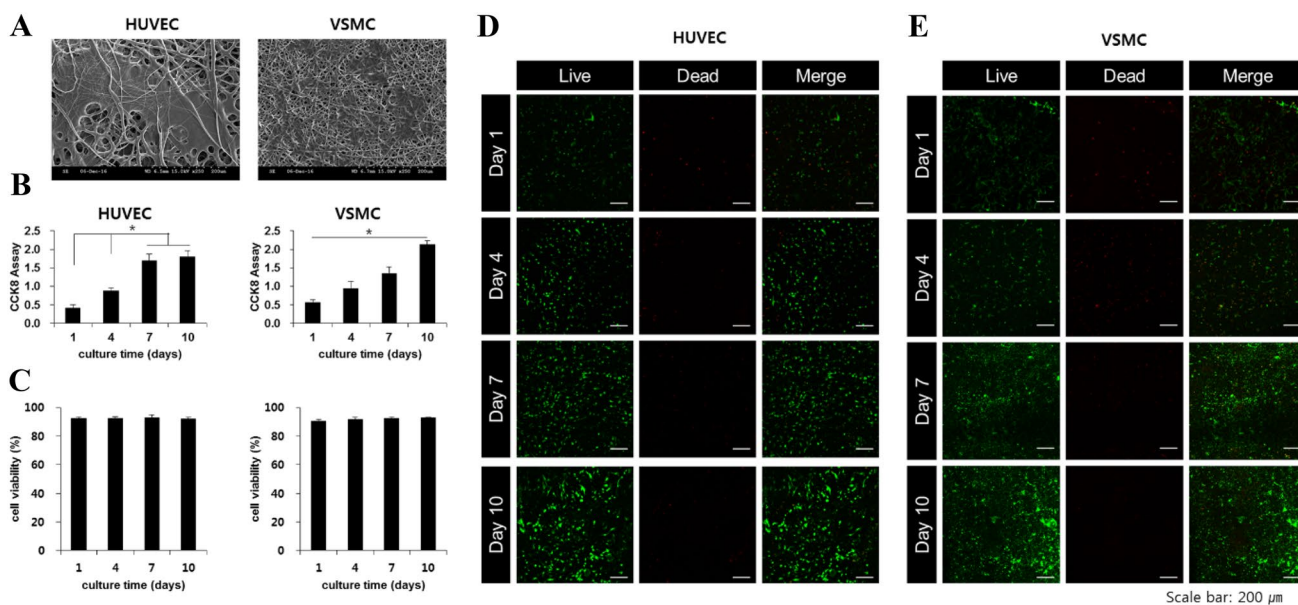


Fig. 5 Cell survival and proliferation on the scaffold. **a** SEM images of ECs and VSMCs attached to the scaffold. **b** ECs and VSMCs proliferation results using CCK8 assay kit. **c**, **d** Live/dead assay results

of ECs or VSMCs on the scaffold (>90% survival rate). **d** Live/dead fluorescent images of HUVECs for culture time (7 days). **e** Live/dead fluorescent images of VSMCs for culture time (7 days)

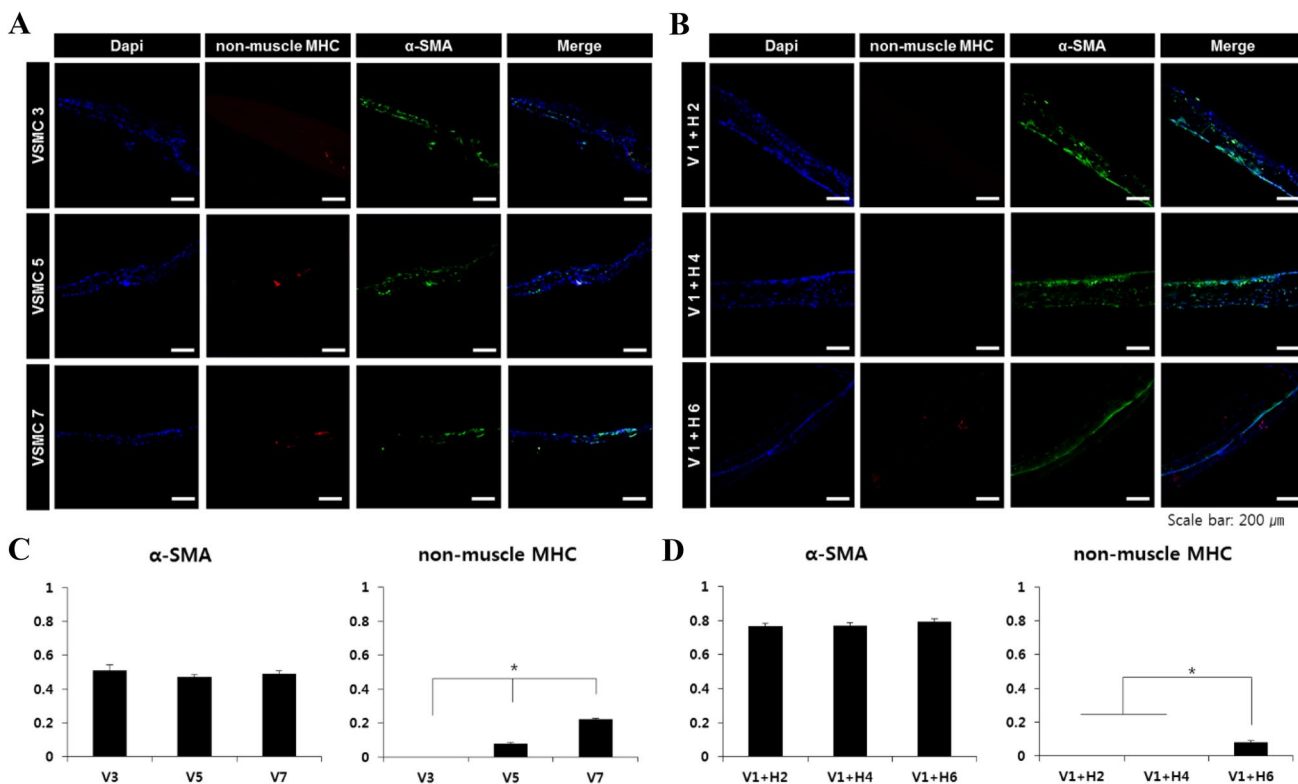


Fig. 6 Phenotype changes of the VSMCs in multi-layer trimmed scaffolds. **a** Staining images of VSMCs single culture on the scaffold. **b** Staining images of co-culture of VSMCs and ECs on the scaffold. **c** Detection levels of α -SMA (contractile type) and non-muscle MHC (synthetic type) at single cultured VSMCs. **d** Detection levels of α -SMA (contractile type) and non-muscle MHC (synthetic type) at co-culture of VSMCs and ECs. (V3: VSMC single cell culture for

3 days, V5: VSMC single cell culture for 5 days, V7: VSMC single cell culture for 7 days. V1+H2: ECs were seeded 1 day after VSMC seeding and stained after 3 days of total culture time. V1+H4: ECs were seeded 1 day after VSMC seeding and stained after 5 days of total culture time. V1+H6: ECs were seeded 1 day after VSMC seeding and stained after 7 days of total culture time.)

(V3: VSMC single cell culture for 3 days, V5: VSMC single cell culture for 5 days, V7: VSMC single cell culture for 7 days. V1 + H2: ECs were seeded 1 day after VSMC seeding and stained after 3 days of total culture time. V1 + H4: ECs were seeded 1 day after VSMC seeding and stained after 5 days of total culture time. V1 + H6: ECs were seeded 1 day after VSMC seeding and stained after 7 days of total culture time.)

3.7 Co-culture of ECs and VSMCs on the Tubular Scaffold

A co-culture of ECs and VSMCs was performed on the tubular scaffold. 3 days after VSMC seeding, the ECs were seeded (Fig. 7). At 6 days after EC seeding, the ECs created a thin layer, which was stained by von Willebrand factor (vWF), an EC marker [18]. On the outside of the EC layer, the VSMCs were shown, which was stained by α -SMA. At this time, MHC was expressed very weakly negligible.

4 Discussion

NPR scaffolds have the unique ability to expand transversely when pulled axially, thereby resulting in a highly-compliant tubular scaffold. A previous study showed that the NPR

design offered a significant advance in the development of highly-compliant vascular grafts [3]. Projection stereolithography was used to 3D-print a planar NPR sheet composed of a photosensitive PEGDA, and it was rolled into a tube [3]. However, the mechanical properties were changed by the overlapped area used to attach the sheet edges. In addition, PEGDA is permitted for limited *in vivo* use. Therefore, in our study, we addressed this limitation by creating a tubular scaffold that demonstrated NPR or PPR behavior by 3D printing on a rotating rod. We successfully fabricated a tubular scaffold with a diameter of 5 mm. We used PCL for the 3D printing and electrospinning. PCL has exceptional bio-compatibility has stimulated extensive research for potential applications in the biomedical field, and the long degradation time (~ 2 years) makes it suitable for long-term applications [19].

A scaffold for an artificial vessel should provide mechanical support, regulate cell activity, provides guide cell migration, and mimic the structure and biological functions of the ECM [20, 21]. Because of the high specific surface area (similar to the ECM structure) and tunable surface morphology, electrospun fibrous scaffolds demonstrate a high potential for engineering various types of tissue, especially vascular vessels [20, 21]. In our study, we added electrospun fibers on to a 3D printed tubular structure, which had NPR or PPR properties, to create a

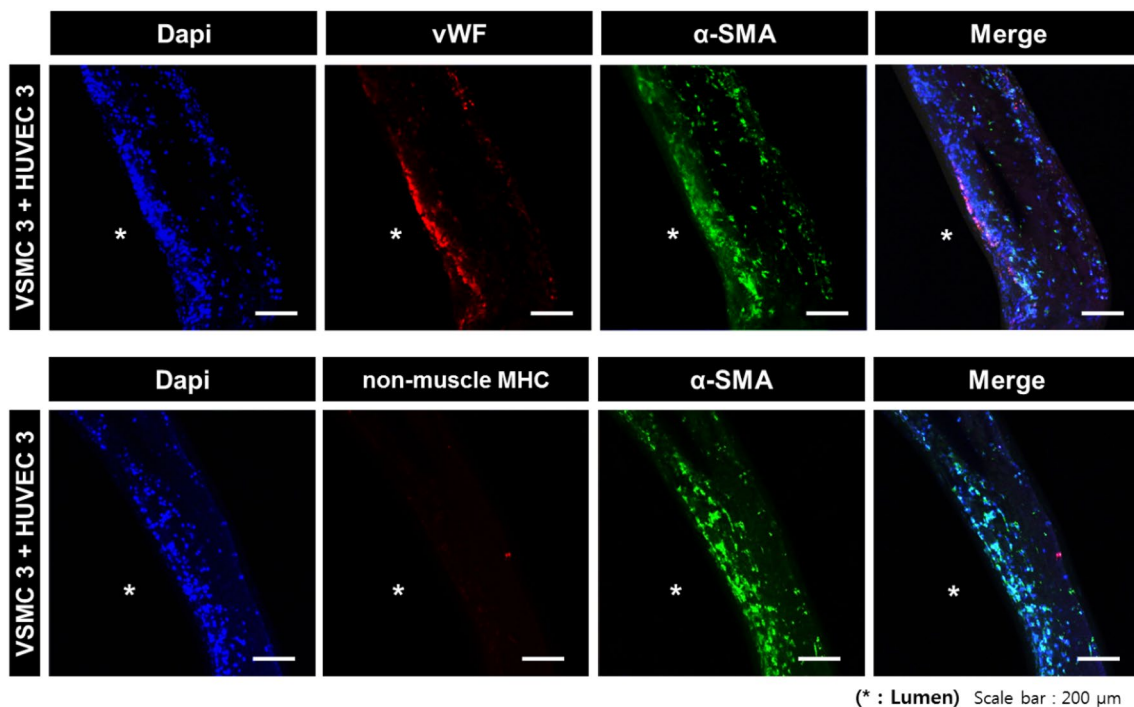


Fig. 7 Co-culture of ECs and VSMCs on the tubular scaffold. (ECs were seeded 3 days (72 h) after VSMC seeding. At 6 days (144 h) after VSMC seeding, the ECs created a thin layer, which were stained

by vWF. Beneath the EC layer, the VSMCs produced a thicker layer, which was stained by α -SMA)

scaffold similar to the biological ECM and enhance proper regeneration of an artificial vessel. When the electrospun fibers were added, the NPR or PPR scaffold maintained their original NPR or PPR properties, and the NPR or PPR properties caused by electrospinning was not severely changed.

It was confirmed that the developed NPR vascular scaffold has about 4 times higher compliance than a PTFE artificial vascular graft used in clinical surgery. This result suggests a solution to the problem of vascular occlusion caused by compliance mismatch through the higher flexibility of the developed scaffold, when an artificial vessel is connected to the artery. Of course, it is true that it has a lower value than that of human femoral artery with 6.0% compliance [16, 22]. However, if the shape, location, size of the NPR patterns, and a line width of unit cells composed of NPR pattern are adjusted, the compliance value could be further improved. These results were consistent with our hypotheses, showing the potential as small diameter blood vessels.

Because the biological blood vessel is composed of three layers and each layer mainly consists of one type of endemic vascular cell (EC, VSMC, and fibroblast cells), the scaffold should enable the development of a similar bionic structure in the *in vitro* cell culture so that it can temporarily perform as a graft substitute after implantation and accomplish blood vessel regeneration *in vivo* [23]. Accordingly, a 3D scaffold that guides the specific vascular cells to the particular sites in the interior and allows the cells to grow and proliferate three-dimensionally inside the scaffold is desirable for an artificial vessel [23].

A combination of microfibers and nanofibers may represent an optimization solution to guide the specific vascular cells to the particular sites. While the nanofibers provide an ECM-like substrate for cell attachment, the microfibers provide sufficient cellular infiltration [1]. Ju et al. used a co-electrospinning technique to fabricate PCL/collagen bilayer scaffolds with an outer layer containing thick fiber that enhanced VSMC infiltration and an inner layer with a thin fiber that facilitated EC attachment [24]. The resulting scaffolds showed endothelialization onto the luminal surface, and the VSMCs penetrated into the outer layer.

In our study, we created luminal electrospun nanosized fibers and outer microsized electrospun fibers. The VSMCs were intended to infiltrate into the outer microsized layer and proliferate to generate a medial layer, which is similar to biological vessels. At first, we evaluated whether the surface of electrospun fiber layer was proper for cell adhesion and proliferation. The results showed that the VSMCs seeded on the scaffold survived and proliferated well for an entire

culture time (10 days). We expected that the ECs seeded on the nanosized fiber could create a thin layer similar to the endothelial layer of biological vessels because the ECs could not infiltrate through the nanosized fiber layer. The ECs on the luminal side of scaffold survived and proliferated well in our study.

It was reported that the small diameter arteries such as coronary artery walls consist of adventitia 200 μm thickness relatively, tunica media 200 μm , and tunica intima of thickness from 100 to 400 μm on average [25]. Based on this report, we made 200 μm thickness of luminal electrospun layer, 200 μm thickness of 3D printed layer, and 400 μm thickness of outer electrospun layer.

The interactions between EC and VSMC are pivotal to blood vessel development and function. EC are in intimate proximity to and communicate with SMC through heterocellular junctions and signaling molecules [26–28]. The VSMC metabolism, differentiation, proliferation, and vasomotion are regulated by the ECs, which have an important role in maintaining a stable environment within the vessel wall and many physiological and pathological processes [29]. The co-culture systems of the ECs and VSMCs enable cellular communication via the growth factors, cytokines, and other soluble mediators secreted by these two types of cells [25].

VSMCs regulate their phenotype in response to environmental, chemical, physical, and mechanical signals, and under normal physiological conditions, VSMCs rarely proliferate [30]. However, these cells can grow rapidly under some pathologic conditions, such as atherosclerosis or intimal hyperplasia [30]. The vascular regeneration of contractile VSMCs on scaffolds may facilitate the production of functional artificial vessels, and their proliferation on scaffolds is essential for generating vascular tissues [30, 31]. However, the uncontrolled proliferation of VSMCs in implanted grafts causes thickening of the vessel walls, intimal hyperplasia, and narrowing of the vessel lumens [30, 31]. In our study, compared to the single cell culture of the VSMCs, where the synthetic-type VSMCs appeared at day 5 of the culture, the time point for the synthetic type to appear was delayed to 7 days of culture by co-culture with the ECs.

For a culture on the vascular scaffold, a uniform cell seeding is challenging owing to the tubular-shaped geometry. On the luminal side, it is difficult to seed the cells with a conventional seeding method, which involves manually seeding the cells with a pipette [20, 32]. This process has shown limited cell adhesion and penetration into the vascular scaffolds, resulting in a low cell seeding efficiency [20, 32]. Thus, we seeded the VSMCs and ECs at different time points for

co-culture. First, the VSMC was seeded to allow the VSMCs to infiltrate through outer microsized fiber layer and migrate even into 3D printed layer of tubular graft. We expected the luminal surface, had nanosized fiber layer which the pores was not big enough for VSMC to pass by, protect VSMC migration into lumen. We confirmed that the synthetic type change of VSMC was decreased when we seeded EC at 1 day after VSMC seeding on trimmed graft. Thus, we seeded EC at 1 day after VSMC seeding on the tubular graft. However, VSMC culture for 1 day was not enough to infiltrate VSMC into the vascular graft differently from trimmed graft culture condition. We made various co-culture condition on the tubular graft and chose the co-culture condition, where the ECs were seeded at 3 days after VSMC seeding.

At day 6 of the co-culture, we successfully generated a thin layer of ECs on the luminal side and minimized the VSMC phenotype changes. The full regeneration of VSMC in the middle layer was not achieved in the time point. It seems that 6 days of culture time was not enough for full regeneration of VSMC. Though we should confirm the full regeneration of middle layer by longer period of culture by a future study, our results showed feasibility that well aligned EC and VSMC layer which was similar with native artery with decreasing synthetic type change of VSMC could achieve by our tubular graft.

In this study, we chose the co-culture condition, where the ECs were seeded 3 days (72 h) after VSMC seeding, for the co-culture on the tubular scaffold. This time point could minimize the synthetic-type phenotype change of the VSMCs and maximize the proliferation of the VSMCs to support the mechanical strength of the vessel in the future. At day 7 of the co-culture, we successfully generated a thin layer of ECs on the luminal side and a proper thickness of the VSMC layer.

5 Conclusions

Our vascular scaffold, which contained NPR properties, would be compatible because it is responsive to blood flow or pressure changes. As a result of compliance measurement, it was confirmed that the compliance value of the NPR tubular structure was higher than that of the PPR and commercial PTFE vascular graft. Furthermore, a compliance value could be further improved by modulating the shape, location, the size of the NPR pattern and line width of a unit cell composed of the NPR pattern. In addition, it is similar to biologic vessels because it contained a thin layer of ECs and a proper thickness of VSMC layers under the EC layer by modulating the electrospun fiber size and

co-culture. Our vascular scaffolds maintained the contractile VSMC phenotype more efficiently using the co-culture, of ECs and VSMCs. Our three layered scaffolds could be used to modulate the compliance of artificial vessels.

Acknowledgements This research was supported by the National Research Foundation of Korea (NRF) (2020R1A2C200652811) and the Gachon University research fund of 2018 (GCU-2018-0367).

Author Contributions C.B.A., J.H.K., K.H.S., and J.W.L. conceived the experiments, C.B.A., J.H.K., J.-H.L. conducted the experiments, K.Y.P., K.H.L., and J.W.L. analyzed the results. K.H.S. and J.W.L. wrote the article. All authors reviewed the manuscript.

Declarations

Conflict of interest The authors declare no competing interests.

References

1. Hasan, A., et al. (2014). Electrospun scaffolds for tissue engineering of vascular grafts. *Acta Biomaterialia*, 10(1), 11–25.
2. Greenwald, S. E., & Berry, C. L. (2000). Improving vascular grafts: the importance of mechanical and haemodynamic properties. *The Journal of Pathology*, 190(3), 292–299.
3. Fozdar, D. Y., et al. (2011). Three-dimensional polymer constructs exhibiting a tunable negative Poisson's ratio. *Advanced Functional Materials*, 21, 2712–2720.
4. Kurane, A., Simionescu, D., & Vyavahare, N. (2007). In vivo cellular repopulation of tubular elastin scaffolds mediated by basic fibroblast growth factor. *Biomaterials*, 28, 2830–2838.
5. Conte, M. S. (1998). The ideal small arterial substitute: a search for the Holy Grail. *FASEB Journal*, 12, 43–45.
6. Popov, E. P. (1990). *Engineering mechanics of solid* (1st ed., pp. 82–83). Prentice Hall.
7. Evans, K. E., et al. (1991). Molecular network design. *Nature*, 353, 124–124.
8. Grima, J. N., & Gatt, R. (2010). Perforated sheets exhibiting negative Poisson's ratios. *Advanced Engineering Materials*, 12, 460–464.
9. Singh, C., Wong, C. S., & Wang, X. (2015). Medical textiles as vascular implants and their success to mimic natural arteries. *Journal of Functional Biomaterials*, 6(3), 500–525.
10. Dora, K. A. (2001). Cell–cell communication in the vessel wall. *Vascular Medicine*, 6, 43–50.
11. Heydarkhan-Hagvall, S., et al. (2003). Co-culture of endothelial cells and smooth muscle cells affects gene expression of angiogenic factors. *Journal of Cellular Biochemistry*, 89(6), 1250–1259.
12. Korff, T., et al. (2001). Blood vessel maturation in a 3-dimensional spheroidal coculture model: direct contact with smooth muscle cells regulates endothelial cell quiescence and abrogates VEGF responsiveness. *FASEB Journal*, 15(2), 447–457.
13. Ahn, H., et al. (2015). Engineered small diameter vascular grafts by combining cell sheet engineering and electrospinning technology. *Acta Biomaterialia*, 16, 14–22.
14. Gaspar, N., et al. (2005). Novel honeycombs with auxetic behavior. *Acta Materialia*, 53, 2439–2445.

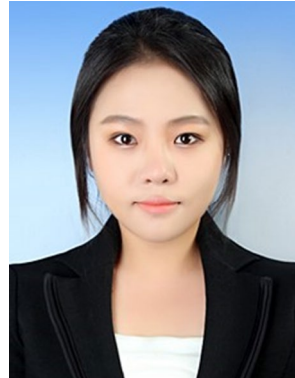
15. Smith, C. W., Grima, J. N., & Evans, K. E. (2000). A novel mechanism for generating auxetic behaviour in reticulated foams: missing rib foam model. *Acta Materialia*, *48*, 4349–4356.
16. Walden, R., et al. (1980). Matched elastic properties and successful arterial grafting. *Archives of Surgery*, *115*(10), 1166–1169.
17. Rensen, S. S., Doevendans, P. A., & van Eys, G. J. (2007). Regulation and characteristics of vascular smooth muscle cell phenotypic diversity. *Netherlands Heart Journal*, *15*(3), 100–108.
18. Pusztaszeri, M. P., Seelentag, W., & Bosman, F. T. (2006). Immunohistochemical expression of endothelial markers CD31, CD34, von Willebrand factor, and Fli-1 in normal human tissues. *Journal of Histochemistry & Cytochemistry*, *54*, 385–395.
19. Ercolani, E., Gaudio, C. D., & Bianco, A. (2015). Vascular tissue engineering of small-diameter blood vessels: reviewing the electrospinning approach. *Journal of Tissue Engineering and Regenerative Medicine*, *9*, 861–888.
20. Pu, J., et al. (2015). Electrospun bilayer fibrous scaffolds for enhanced cell infiltration and vascularization in vivo. *Acta Biomaterialia*, *13*, 131–141.
21. Xu, C. Y., et al. (2004). Aligned biodegradable nanofibrous structure: a potential scaffold for blood vessel engineering. *Biomaterials*, *25*, 877–886.
22. Gooch, K. J., et al. (2018). Biomechanics and mechanobiology of saphenous vein grafts. *Journal of Biomechanical Engineering*, *140*, 020804.
23. Ye, L., et al. (2015). The fabrication of double layer tubular vascular tissue engineering scaffold via coaxial electrospinning and its 3D cell coculture. *Journal of Biomedical Materials Research Part A*, *103*, 3863–3871.
24. Ju, Y. M., et al. (2010). Bilayered scaffold for engineering cellularized blood vessels. *Biomaterials*, *31*, 4313–4321.
25. Ozolanta, I., et al. (1998). Changes in themechanical properties, biochemical contents and wall structure of the human coronary arteries with age and sex. *Medical Engineering & Physics*, *20*, 523–533.
26. Xiang, W., et al. (2017). Co-cultures of endothelial cells and smooth muscle cells affect vascular calcification. *International Journal of Clinical and Experimental Medicine*, *10*(6), 9038–9046.
27. Williams, C., & Wick, T. M. (2005). Endothelial cell-smooth muscle cell co-culture in a perfusion bioreactor system. *Annals of Biomedical Engineering*, *33*, 920–928.
28. Davies, P. F. (1986). Vascular cell interactions with special reference to the pathogenesis of atherosclerosis. *Laboratory Investigation*, *55*, 5–24.
29. Davies, P. F., et al. (1988). Endothelial communication. *State of the art lecture. Hypertension*, *11*, 563–572.
30. Chan-Park, M. B., et al. (2009). Biomimetic control of vascular smooth muscle cell morphology and phenotype for functional tissue engineered small-diameter blood vessels. *Journal of Biomedical Materials Research Part A*, *88*, 1104–1121.
31. Vatanhaha, E., Prabhakaran, M. P., & Ramakrishnan, S. (2017). Impact of electrospun Tecophilic/gelatin scaffold biofunctionalization on proliferation of vascular smooth muscle cells. *Scientia Iranica*, *24*(6), 3458–3465.
32. Madden, L. R., et al. (2010). Proangiogenic scaffolds as functional templates for cardiac tissue engineering. *Proceedings of the National Academy of Science of the United States of America*, *107*(34), 15211–15216.



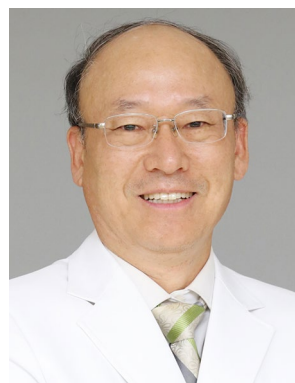
Chi Bum Ahn received his Ph.D degree of the Department of Biomedical Engineering at Korea University in South Korea in 2011. His research interests include 3D printing technology and its application to biomedical field such as medical device, tissue engineering.



Joo Hyun Kim received her Ph.D degree of the Department of Health Sciences and Technology at Gachon University in South Korea in 2020. Her research interests include 3D printing technology, tissue engineering and stem cell application.



Ji-Hyun Lee received her Ph.D degree of the Department of Dentistry at Kyungpook National University in South Korea in 2013. Her research interests include stem cell therapy and tissue engineering.



Kook Yang Park received his PhD at the Department of Thoracic surgery of Seoul National University Medical College in 1988. He is currently a professor and active surgeon in Cardiothoracic surgery of Gil Medical Center, Gachon University.

Publisher's Note Springer Nature remains neutral with regard to jurisdictional claims in published maps and institutional affiliations.



Kuk Hui Son is an associate professor in the Department of Thoracic and Cardiovascular Surgery, Gil Medical Center at Gachon University since 2013. Her research interests include regeneration medicine especially related with cardiovascular disease.



Jin Woo Lee is an associate professor in the Department of Molecular Medicine at Gachon University since 2014. His research interests are realization of 3D micro-environment using 3D printing, and synthesis and modification of biomaterials.